

RSC Advances



This is an *Accepted Manuscript*, which has been through the Royal Society of Chemistry peer review process and has been accepted for publication.

Accepted Manuscripts are published online shortly after acceptance, before technical editing, formatting and proof reading. Using this free service, authors can make their results available to the community, in citable form, before we publish the edited article. This *Accepted Manuscript* will be replaced by the edited, formatted and paginated article as soon as this is available.

You can find more information about *Accepted Manuscripts* in the [Information for Authors](#).

Please note that technical editing may introduce minor changes to the text and/or graphics, which may alter content. The journal's standard [Terms & Conditions](#) and the [Ethical guidelines](#) still apply. In no event shall the Royal Society of Chemistry be held responsible for any errors or omissions in this *Accepted Manuscript* or any consequences arising from the use of any information it contains.

ARTICLE

Hierarchical TiO₂ spheres decorated with Au nanoparticles for visible light hydrogen production

Cite this: DOI: 10.1039/x0xx00000x

Guoqiang Zhang,^{ab} Zhao Zhao,^{ab} Huaqiao Tan,^a Haifeng Zhao,^a Dan Qu,^{ab} Min Zheng,^a Weixing Yu^c and Zaicheng Sun^{c*}

Received 00th January 2012,

Accepted 00th January 2012

DOI: 10.1039/x0xx00000x

www.rsc.org/

Abstract. Hierarchical TiO₂ spheres composed of nanosheets are successfully synthesized via a simple solvothermal route. TiO₂ spheres with high surface area (~100 m²/g) exhibit excellent photocatalytic activity. Au nanoparticles are loaded on the surface of TiO₂ nanosheets through anchor molecules – thioglycolic acid. The LSPR absorption band at ~550 nm of Au nanoparticles is clearly observed in the diffusion reflective UV-Vis spectra. H₂ production results shows the TiO₂ spheres have higher photocatalytic activity than commercial P25 TiO₂. After loading with Au nanoparticles, TiO₂-Au spheres display 27.6 μmol/(g.h) of H₂ production rate under visible light irradiation (λ>420 nm) because the localized surface plasmon resonance (LSPR) of Au nanoparticles enhances the visible light absorption. Furthermore, the H₂ production rate could be improved to 92.4 μmol/(g.h) for TiO₂ spheres loaded with both Au and Pt nanoparticles. Based on these results, we propose the possible mechanism. Under UV light, TiO₂ absorbs UV light and generates excited electron, passing to Au nanoparticles for H₂ production. In the case of visible light irradiation, the hot electrons are generated from Au nanoparticles due to LSPR effect. And then the hot electrons are transferred from Au nanoparticles to TiO₂ and cocatalyst Pt nanoparticles for H₂ generation.

Introduction

Titanium dioxide (Titania, TiO₂) is one of the most widely used semiconducting oxide materials and has a wide range of applications including bio-separation, sensors, energy storage, solar cells, catalysis and photocatalysis.¹⁻⁷ TiO₂ offers a number of advantageous characteristics including low cost, relatively high photocatalytic activity, low toxicity, and high chemical and optical stability. Since the discovery of hydrogen production from water through electrochemical photolysis,⁸ TiO₂ has been intensively studied and used as a photocatalyst in both fundamental research and practical applications.⁹⁻¹¹ Due to its large band gap (E_g = 3.0-3.2 eV), it can absorb UV light and generate electron (e⁻) and hole (h⁺) pairs which can induce a variety of red-ox reactions. Over the past few decades, tremendous efforts have been devoted to improving the catalytic activity of TiO₂-based photocatalysts with well controlled characteristics.¹²⁻¹⁴ However, weak absorption in visible region lies still on the way for the practical applications like solar water splitting. Generally, a few routes have been used for improving the absorption of TiO₂ in visible region. Firstly, doping TiO₂ with metal (like Fe³⁺, Cr³⁺, Ti³⁺ etc.) or non-metal (for example C, N, S and so on) will narrow the band gap.^{11, 15-18} Secondly, sensitizing TiO₂ with narrow band gap quantum dots or dye molecules, which absorb visible light and inject electron or hole into TiO₂, improves the overall photocatalytic capability of TiO₂.¹⁹⁻²³

Another promising route to enhance the photocatalytic performance of TiO₂ is to decorate the surface with noble metal

nanoparticles (e.g. Ag, Au, Pt, and Pd).²⁴⁻²⁸ It has been shown that the presence of the noble metal nanoparticles can effectively shift the Fermi level of TiO₂, which results in the enhanced photocatalytic efficiency.^{24, 29} On the other hand, the localized surface plasmon resonance (LSPR) of noble metal nanoparticles also enhances the absorption in the visible region of TiO₂. Kamat *et al.* investigated the size dependence of Au-TiO₂ nanocomposites and found that small Au particles lead to large apparent Fermi level shift (20 mV for 8-nm diameter and 40 mV for 5-nm and 60 mV for 3-nm gold nanoparticles), which improves the photoinduced charge separation.²⁴ In traditional way, adding the noble metal salt into TiO₂ sol-gel precursor and photo-reducing the noble metal salts, it is hard to avoid the aggregation of gold nanoparticle to form big particles.³⁰⁻³² Preparation of TiO₂ hierarchical nanostructures loaded with Au nanoparticles are highly desired. Recently, Lou *et al.* reported the hierarchical TiO₂ spheres composed in nanosheets with high surface area (~100 m²/g) and high reactive (001) facet.³³ On the other hand, this hierarchical TiO₂ spheres have both accessible macropores from intersheets and mesopores from the packing of nanoparticles within nanosheets.

Herein, hierarchical TiO₂ spheres composed in nanosheets were synthesized via modified Lou's route. Based on the hierarchical TiO₂ spheres, we developed a facile method to load Au nanoparticles on the surface of TiO₂ nanosheets by introducing an anchor molecule thioglycolique acid (TGA), which effectively controls the size of Au nanoparticles with ~5 nm in diameter. The obtained TiO₂-Au spheres possess the

following advantages: i) hierarchical structure shows high photocatalytic performance from large surface area; ii) the LSPR of Au nanoparticles enhances the visible light absorption and improves the photocatalytic performance of TiO₂ in the visible light region. H₂ production experiments indicate that the TiO₂-Au spheres show a high photocatalytic performance in both UV and visible region due to Au nanoparticles on the TiO₂ surface. That makes TiO₂ spheres decorated with Au nanoparticles as a high active visible-light photocatalyst.

Results and discussion

Firstly, the large scale of TiO₂ spheres were prepared according to Lou's report with a modification.³³ Fig. S1 shows field-emission scanning electron microscopy (FE-SEM) images of the obtained TiO₂ spheres, which size can be tuned from 400-800 nm in diameter by reaction conditions. Close inspection images disclose that the TiO₂ spheres are composed of TiO₂ nanosheets, which is about 10 nm in thickness. High resolution TEM image displays that the nanosheets are composed of TiO₂ nanoparticles with ~ 6 nm of diameter after long time calcination. The crystalline phase of these TiO₂ spheres can be transferred into anatase phase under calcination at 400 °C for 2-4 hours. The XRD patterns as shown in Fig. 3A, the calcined TiO₂ spheres exhibit a typical anatase crystalline phase pattern (JCPDS No. 21-1272). To obtain Au nanoparticles on the TiO₂ nanosheets surface, here we used an anchor molecule TGA, which has two functional groups, carboxyl group (-COOH) and thiol group (-SH). The COOH group makes the anchor molecules attach on the TiO₂ surface. The thiol group on the other side will expose on the surface. Au complexes (Au (TGA)) forms between TGA and HAuCl₄ with the addition of HAuCl₄. Then Au nanoparticles form by adding into fresh NaBH₄ solution. The anchor molecule TGA has a key role for the Au nanoparticles formation. It can effectively prevent from the aggregation of Au.

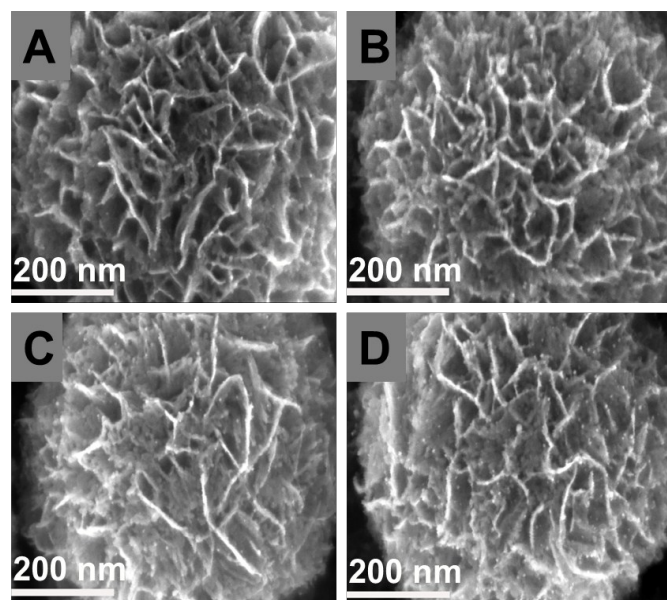


Fig. 1 Field emission scanning electron microscopy (FE-SEM) images of TiO₂ spheres decorated with different amount of Au nanoparticles. A, 1.07 wt% (TiO₂-Au1), B, 2.00 wt% (TiO₂-Au2), C, 2.43 wt% (TiO₂-Au3) and D 2.82 wt% (TiO₂-Au4) measured from EDAX.

Fig. 1 show the FE-SEM images of TiO₂ spheres decorated with Au nanoparticles. After loading Au nanoparticles, the morphology of TiO₂ spheres is well kept. With the increase of HAuCl₄ amount, the more HAuCl₄ can be adsorbed on the TGA modified surface of TiO₂ spheres. After reducing, Au nanoparticles are denser on the surface of TiO₂ spheres. The energy dispersive x-ray analysis (EDAX, Fig. S2 and S3) proves the existence of Au. According to EDAX results, the weight fraction of loaded Au nanoparticles increases from 1.07, 2.00, 2.43 to 2.82 wt% by adding 5, 10, 20 and 30 mL of 1.0 mmol/L HAuCl₄·3H₂O solution into TiO₂ sphere dispersion for samples TiO₂-Au1, 2, 3, and 4, respectively. Fig. 2 display transmission electron microscopy (TEM) images of TiO₂ spheres decorated with Au nanoparticles. Low magnification TEM image (Fig. 2A) clearly shows the TiO₂ sphere with nanosheets structures. High resolution TEM images exhibit that 0.35 and 0.24 nm are characteristic lattice fringe space of anatase TiO₂ (101) and Au (111) nanoparticles, respectively. That reveals the uniform Au nanoparticles with ~5 nm in diameter are attached on the TiO₂ nanosheets. In addition, the TiO₂ nanosheets are composed of TiO₂ nanoparticles with diameter of 6.01 ± 1.61 nm (Fig. 2C and D).

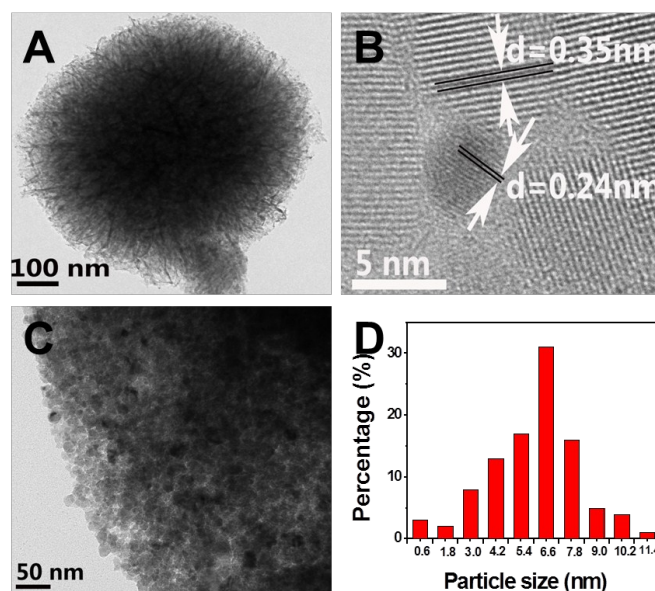


Fig. 2 Transmission electron microscopy (TEM) images of TiO₂ spheres loaded with 2.43 wt% Au nanoparticles (A, C). B is the high resolution TEM image of TiO₂ loaded with Au nanoparticles. 0.35 nm and 0.24 nm are characteristic lattice fringe space of anatase TiO₂ (101) and Au (111) nanoparticles. The histogram of TiO₂ nanoparticles calculated from TEM images of Fig. 2C.

Fig. 3A displays the X-Ray diffraction patterns of TiO₂ loaded with different amount of Au nanoparticles. It clearly shows the diffraction peaks at 25.3, 37.8, 48.0 degree, which are related to the (101), (004), (200) of anatase phase TiO₂ (JCPDS no. 21-1272). According to the Scherrer equation, the TiO₂ nanocrystal size was calculated to be 10 nm using (101) reflection peak. It is consistent with the diameter of TiO₂ measured from TEM images. Diffused reflective UV-Vis spectroscopy is presented in the Figure 3B. Compared with TiO₂ spheres, a broad absorption band at ~550 nm, related to the plasmon resonance of Au, is observed for the TiO₂ spheres loaded with Au nanoparticles. The hierarchical TiO₂ spheres

exhibit high surface area. The Brunauer–Emmett–Teller (BET) surface area and pore size of the TiO₂ spheres are characterized using nitrogen adsorption–desorption isotherm shown in Fig. 3C and D. It gives a type-IV isotherm with a type-H3 hysteresis loop, indicating a mesoporous structure.³⁴ The BET surface area of TiO₂ spheres with and without Au nanoparticles are determined to be 97 and 103 m²/g, respectively. According to previous reports,³⁵ a bimodal mesopore size distribution was implied in this type of hysteresis loop. The hysteresis loop in the lower relative pressure range (0.4 < P/P₀ < 0.8) is attributed to the mesopores from the packing of nanoparticles within nanosheets and that in the high relative pressure range (0.8 < P/P₀ < 1.0) is related to the macropores from intersheets.

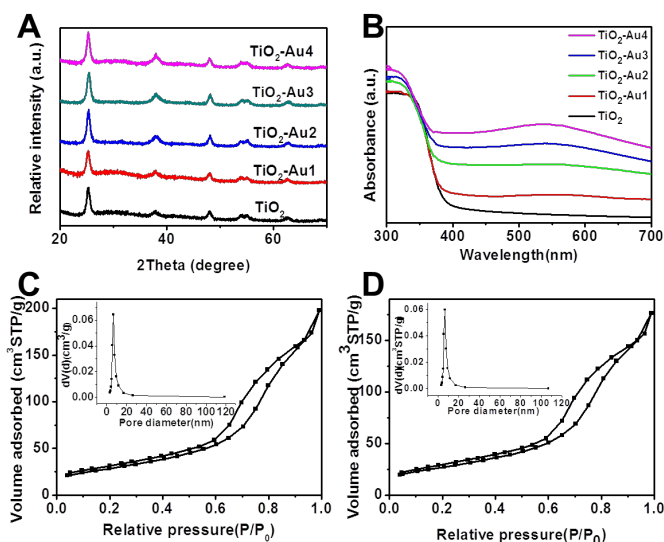


Fig. 3 X-ray diffraction pattern (A) and diffusion reflection UV-Vis spectra (B) of TiO₂ spheres loaded different amount of Au nanoparticles (TiO₂-Au1-4 for Au weight fraction 1.07, 2.00, 2.43, 2.82 wt% respectively). C and D are the N₂ sorption curves of TiO₂ sphere without and with Au nanoparticles, respectively. Insets are the pore size distribution curves.

TiO₂ spheres exhibit high photocatalytic activity compared with commercial P25 TiO₂. Fig. S4A shows the H₂ production of TiO₂ spheres and P25 TiO₂ loaded with 1 wt% Pt as cocatalyst under UV-Vis light (300 W Xe lamp). The H₂ evolution rate is about 335 and 204 μmol/hour for 10 mg TiO₂ sphere and P25 TiO₂, respectively. The main reason is that TiO₂ spheres have larger surface area than P25 TiO₂ (~50 m²/g). No H₂ production is observed for 10 mg of TiO₂ sphere under UV-visible light. (Fig S4B). It exhibits obvious photocatalytic activity after loading Au nanoparticles. The H₂ production rate is ~23.9, 53.6, 165 and 87.3 μmol/hour for 10 mg sample of TiO₂ - Au1, 2, 3, and 4, respectively. The photocatalytic activity reaches maximum when the Au nanoparticles amount is about 2.43 wt% (TiO₂-Au3). These results indicate that Au nanoparticles could work as a cocatalyst for H₂ production. TiO₂ adsorbs UV light and the electron was excited from valance band (VB) to conduction band (CB), then the photogenerated electron can inject into Au nanoparticles. The proton accepts the electron and forms H₂.

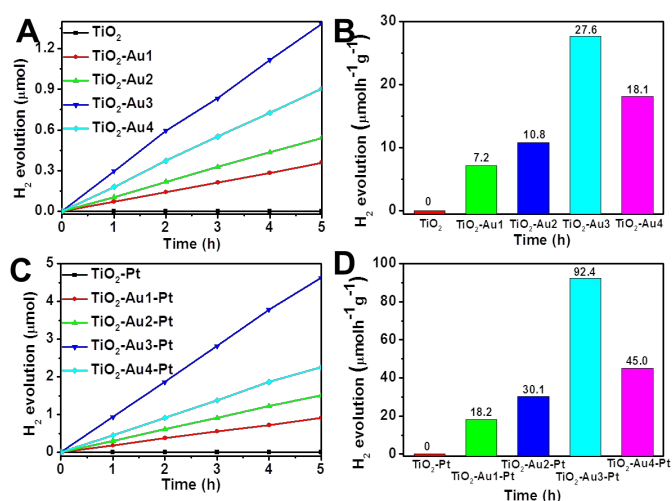
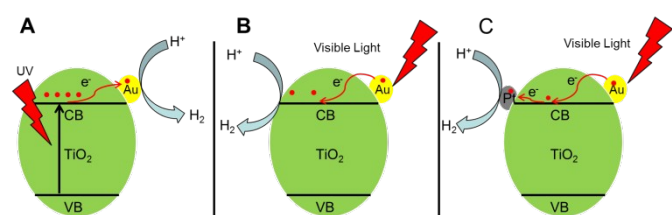


Fig. 4 (A) H₂ production of TiO₂ spheres loaded with different amount Au nanoparticles under visible light ($\lambda > 420$ nm). (B) Normalized H₂ production rate of TiO₂ sphere with Au nanoparticles. (C) H₂ production of TiO₂ spheres loaded with Au and Pt nanoparticles under visible light ($\lambda > 420$ nm). (D) Normalized H₂ production rate of TiO₂ spheres loaded Au and Pt nanoparticles.

Fig. 4 shows H₂ production rate of TiO₂ sphere with different amount Au nanoparticles under visible light ($\lambda > 420$ nm) in presence and absence of Pt cocatalyst. No H₂ is produced from the pure TiO₂ sphere without loading Au nanoparticles. That indicates that TiO₂ spheres have no response to the visible light. Figure S5 shows TiO₂ spheres loaded both Au and Pt nanoparticles. When Au nanoparticles are attached onto the TiO₂ sphere surface, H₂ is detected. That means that Au nanoparticles absorb the visible light, generate hot electron due to the LSPR effect and transfer hot electron to TiO₂ for H₂ generation. The H₂ evolution rate increases with the increasing of Au nanoparticles amount. However, too much amount of Au nanoparticles (2.84 wt%) results in a decrease of H₂ production rate. The optimal loading amount of Au nanoparticles is about 2.43 wt% and H₂ production rate is about 27 μmol/(g.h). Pt is often chosen as a cocatalyst to lower the over potential of H₂O splitting. Furthermore, when the cocatalyst Pt nanoparticles are loaded onto the TiO₂-Au spheres via photo-reduction reaction, the H₂ production rate has obvious improvement. The H₂ production rate increases from 27 μmol/(g.h) to 92 μmol/(g.h), which is about 3 folds improvement.



Scheme 1. Possible photocatalytic H₂ production mechanism of TiO₂-Au under full spectrum light (A) and visible light ($\lambda > 420$ nm), where B is TiO₂-Au and C is TiO₂-Au and Pt nanoparticles.

Based on the above results, we propose the following mechanism for TiO₂-Au composites (Scheme 1). Under UV light illumination, TiO₂ adsorbs light and is excited to generate exciton. The electron is transferred to Au nanoparticles, which work as cocatalyst to promote H₂ generation (Scheme 1A). It is

known that a Schottky barrier is formed at the Au-TiO₂ interface when Au nanoparticles make direct physical contact with TiO₂.³⁶ Upon excitation of the Au SPR with $\lambda > 420$ nm, intense SPR-enhanced EM field are generated on the surface of Au nanoparticles, increasing the yield of interfacial “hot electrons”. That will induce efficient transfer of “hot electrons” to the CB of TiO₂. The Schottky barrier at the interface also helps the transferred “hot electrons” accumulating in the TiO₂ CB, preventing them from traveling back to Au nanoparticles. Since no holes are generated in the valence band (VB) of TiO₂ under $\lambda > 435$ nm excitation, the transferred “hot electrons” in the TiO₂ CB should have much longer lifetimes, fostering the reduction of H₂O to produce H₂.^{37,38} Further, the reduction of H₂O is promoted by the loading of cocatalyst Pt nanoparticle. The “hot electron” is transferred from Au nanoparticle to the CB of TiO₂, then further to the Pt nanoparticles. Pt nanoparticles prefer to adsorb the proton and lower the over potential of H₂O reduction.³⁹ The hot electrons prefer transfer from Au nanoparticles to Pt nanoparticles where hydrogen evolution occurs. That is the reason why H₂ production rate has an obvious improvement after loading Pt nanoparticles.

Conclusions

In summary, we have loaded Au nanoparticles on the surface of TiO₂ spheres through anchor molecules thioglycolic acid. SEM and TEM disclosed that Au nanoparticles are well dispersed on the surface of TiO₂ sphere. Due to TiO₂ spheres are composed of nanosheets, it possesses relatively large surface area (~ 100 m²/g), which is beneficial to the photocatalytic performance. TiO₂ spheres exhibit high photocatalytic H₂ production rate (165 μ mol/hour for 10 mg of TiO₂-Au₃) under full spectrum light. The TiO₂ spheres loaded with Au nanoparticles also shows good photocatalytic activity under visible light illumination due to the LSPR effect of Au nanoparticles. The photocatalytic performance could be further improved to 97 μ mol/hour for 10mg TiO₂-Au₃ by loading the cocatalyst Pt nanoparticle on the TiO₂.

Experimental

Chemicals and Materials

HAuCl₄.3H₂O (AR), NaBH₄ (98%), thioglycolic acid (TGA, AR, 90%), diethylenetriamine (DETA, 99%), and titanium isopropylate (TIP, 98%) were purchased from Aladdin Reagent Company. Methanol (AR), isopropanol (AR) was purchased from Beijing Chemical Reagent Company. All chemicals were used without any further purification.

Synthesis of TiO₂ sphere

At room temperature, the 380 mL of isopropanol was mixed with 300 L of DETA and stirred for 30 min. Then the 12.5 mL of TIP was injected with mixture slowly. The above solution was transferred into a 500 mL Teflon lined stainless steel autoclave and was heated to 200 °C for 48 h in an electric oven. Following this, the reaction was naturally cooled to room temperature. The as-prepared samples were washed with ethanol to remove remaining organic impurity and dried at 70 °C for 12 h in an electric oven. Finally, the samples were annealed at 400 °C for 4 h to form the crystal phase of TiO₂.

Synthesis of TiO₂-Au

At room temperature, the 80 mg of TiO₂ sphere was dispersed into 10 mL of deionized water. 100 μ L of TGA was added into the mixture and stirred for 6 h to make TGA adsorb on TiO₂ sphere surface. Then the above mixture was centrifuged at 9000 rpm for 15 min to remove free TGA molecules. Then, 5, 10, 20 and 30 mL of 1.0 mmol/L HAuCl₄.3H₂O solution was added into TiO₂ spheres dispersion and stirred for 6 h away from light to make gold ion bonded with TGA. Then the mixture was centrifuged at 9000 rpm for 15 min to remove free gold ion. 5mL of 0.1mol/L NaBH₄ solution was injected rapidly and stirred at 1000 rpm. The as-prepared samples were centrifuged and washed with deionized water. Finally, the samples were dried at 70 °C for 12 h.

Characterizations

The Brunauer-Emmett-Teller (BET) specific surface area was measured using a Micromeritics Gemini V Surface Area and Pore Size Analyzer. Scanning electron microscope (SEM) images were measured on JEOL JSM 4800F. Transmission electron microscope (TEM) images were taken using an FEI Tecnai G2 operated at 200 kV. The UV-Vis absorption spectra were recorded on a UV-3600 UV-Vis-NIR scanning spectrophotometer (Shimadzu). The crystalline structure was recorded by using an X-ray diffractometer (XRD) (Bruker AXS D8 Focus), using Cu K_a radiation ($\lambda=1.54056$ Å).

Photocatalytic Activity Measurements

10mg of TiO₂-Au photocatalyst was placed into an aqueous methanol solution (120 ml, 25 vol%) in a closed gas circulation system (Perfect Light Company Labsolar-III (AG)). The UV-visible light irradiations were obtained from a 300 W Xe lamp (Perfect Light Company Solaredge 700) without and with a UVCUT-420 nm filter (CE Aulight .Inc). The evolved gases were detected in situ by using an online gas chromatograph. (GC-2014C, Shimadzu) equipped with a thermal conductivity detector (TCD). To obtain TiO₂-Au-Pt photocatalyst, 10mg of TiO₂-Au photocatalyst loaded with 1.0 wt% Pt (H₂PtCl₆) was placed into an aqueous methanol solution in a closed gas circulation system. Before collecting the evolution gas, the reaction was irradiated with UV-Vis light over an hour for reduction Pt nanoparticles onto the TiO₂-Au samples.

Acknowledgements

The authors thank the National Natural Science Foundation of China (No. 21301166, 21201159, and 61361166004), Science and Technology Department of Jilin Province (No. 20130522127JH, and 20121801) are gratefully acknowledged. Z. S. thanks the support of the “Hundred Talent Program” of CAS. Supported by open research fund program of State Key Laboratory of Luminescence and Applications (CIOMP, CAS) and Key Laboratory of Functional Inorganic Material Chemistry (Heilongjiang University), Ministry of Education, P. R. China.

Notes and references

^a State Key Laboratory of Luminescence and Applications, Changchun Institute of Optics, Fine Mechanics and Physics, Changchun, 130033, Jilin, P. R. China. Email: sunzc@ciomp.ac.cn

^b University of Chinese Academy of Sciences, Beijing, P. R. China.

^c Institute of Micro and Nano Optics, College of Optoelectronic Engineering, Shenzhen University, Shenzhen 518060, China

† Electronic Supplementary Information (ESI) available: more SEM, EDAX, H₂ production of TiO₂ spheres. See DOI: 10.1039/b000000x/

1. X. Chen and S. S. Mao, *Chem. Rev.*, 2007, **107**, 2891-2959.
2. M. Graetzel, R. A. J. Janssen, D. B. Mitzi and E. H. Sargent, *Nature*, 2012, **488**, 304-312.
3. J. Du, J. Qi, D. Wang and Z. Tang, *Energy Environ. Sci.*, 2012, **5**, 6914-6918.
4. K. Nakata and A. Fujishima, *J. Photoch. Photobio. C*, 2012, **13**, 169-189.
5. Q. Zhang, E. Uchaker, S. L. Candelaria and G. Cao, *Chem. Soc. Rev.*, 2013, **42**, 3127-3171.
6. T. Froschl, U. Hormann, P. Kubiak, G. Kucerova, M. Pfanzelt, C. K. Weiss, R. J. Behm, N. Husing, U. Kaiser, K. Landfester and M. Wohlfahrt-Mehrens, *Chem. Soc. Rev.*, 2012, **41**, 5313-5360.
7. H. G. Moon, Y.-S. Shim, H. W. Jang, J.-S. Kim, K. J. Choi, C.-Y. Kang, J.-W. Choi, H.-H. Park and S.-J. Yoon, *Sens. Actuators B Chem.*, 2010, **149**, 116-121.
8. A. Fujishima and K. Honda, *Nature*, 1972, **238**, 37-38.
9. X. Chen, S. Shen, L. Guo and S. S. Mao, *Chem. Rev.*, 2010, **110**, 6503-6570.
10. X. Chen, L. Liu, P. Y. Yu and S. S. Mao, *Science*, 2011, **331**, 746-750.
11. F. Zuo, K. Bozhilov, R. J. Dillon, L. Wang, P. Smith, X. Zhao, C. Bardeen and P. Feng, *Angew. Chem., Inter. Ed.*, 2012, **51**, 6223-6226.
12. J. Lee, M. Christopher Orilall, S. C. Warren, M. Kamperman, F. J. DiSalvo and U. Wiesner, *Nat. Mater.*, 2008, **7**, 222-228.
13. M. Yin, Y. Cheng, M. Liu, J. S. Gutmann and K. Müllen, *Angew. Chem., Inter. Ed.*, 2008, **47**, 8400-8403.
14. H. G. Yang, C. H. Sun, S. Z. Qiao, J. Zou, G. Liu, S. C. Smith, H. M. Cheng and G. Q. Lu, *Nature*, 2008, **453**, 638-641.
15. W. Choi, A. Termin and M. R. Hoffmann, *J. Phys. Chem.*, 1994, **98**, 13669-13679.
16. E. Borgarello, J. Kiwi, M. Graetzel, E. Pelizzetti and M. Visca, *J. Am. Chem. Soc.*, 1982, **104**, 2996-3002.
17. R. Asahi, T. Morikawa, T. Ohwaki, K. Aoki and Y. Taga, *Science*, 2001, **293**, 269-271.
18. D. Pan, J. Zhang, Z. Li, C. Wu, X. Yan and M. Wu, *Chem. Commun.*, 2010, **46**, 3681-3683.
19. D. R. Baker and P. V. Kamat, *Adv. Funct. Mater.*, 2009, **19**, 805-811.
20. H. Park, W. Choi and M. R. Hoffmann, *J. Mater. Chem.*, 2008, **18**, 2379-2385.
21. C. Karakaya, Y. Türker and Ö. Dag, *Adv. Funct. Mater.*, 2013, **23**, 4002-4010.
22. E. Bae and W. Choi, *Environ. Sci. Technol.*, 2002, **37**, 147-152.
23. N. Shamim and K. Sharma Virender, eds., *Sustainable Nanotechnology and the Environment: Advances and Achievements*, American Chemical Society, 2013.
24. V. Subramanian, E. E. Wolf and P. V. Kamat, *J. Am. Chem. Soc.*, 2004, **126**, 4943-4950.
25. Y. Lai, Y. Tang, J. Gong, D. Gong, L. Chi, C. Lin and Z. Chen, *J. Mater. Chem.*, 2012, **22**, 7420-7426.
26. R. Su, R. Tiruvalam, Q. He, N. Dimitratos, L. Kesavan, C. Hammond, J. A. Lopez-Sanchez, R. Bechstein, C. J. Kiely, G. J. Hutchings and F. Besenbacher, *ACS Nano*, 2012, **6**, 6284-6292.
27. H. Li, Z. Bian, J. Zhu, Y. Huo, H. Li and Y. Lu, *J. Am. Chem. Soc.*, 2007, **129**, 4538-4539.
28. C. Zhou, L. Shang, H. Yu, T. Bian, L.-Z. Wu, C.-H. Tung and T. Zhang, *Cataly. Today*, 2014, **225**, 158-163.
29. K. Mogyorósi, Á. Kmettykó, N. Czirbus, G. Veréb, P. Sipos and A. Dombi, *React. Kinet. Catal. Lett.*, 2009, **98**, 215-225.
30. M. Epifani, C. Giannini, L. Tapfer and L. Vasanelli, *J. Am. Ceram. Soc.*, 2000, **83**, 2385-2393.
31. S. C. Chan and M. A. Barteau, *Langmuir*, 2005, **21**, 5588-5595.
32. X. Z. Li and F. B. Li, *Environ. Sci. Technol.*, 2001, **35**, 2381-2387.
33. J. S. Chen, Y. L. Tan, C. M. Li, Y. L. Cheah, D. Luan, S. Madhavi, F. Y. C. Boey, L. A. Archer and X. W. Lou, *J. Am. Chem. Soc.*, 2010, **132**, 6124-6130.
34. M. Kruk and M. Jaroniec, *Chem. Mater.*, 2001, **13**, 3169-3183.
35. K. Kaneko, *J. Membr. Sci.*, 1994, **96**, 59-89.
36. Y. K. Lee, C. H. Jung, J. Park, H. Seo, G. A. Somorjai and J. Y. Park, *Nano Lett.*, 2011, **11**, 4251-4255.
37. J. S. DuChene, B. C. Sweeny, A. C. Johnston-Peck, D. Su, E. A. Stach and W. D. Wei, *Angew. Chem., Inter. Ed.*, 2014, **53**, 7887-7891.
38. K. Qian, B. C. Sweeny, A. C. Johnston-Peck, W. Niu, J. O. Graham, J. S. DuChene, J. Qiu, Y.-C. Wang, M. H. Engelhard, D. Su, E. A. Stach and W. D. Wei, *J. Am. Chem. Soc.*, 2014, **136**, 9842-9845.
39. D. Duonghong, E. Borgarello and M. Graetzel, *J. Am. Chem. Soc.*, 1981, **103**, 4685-4690.

Graphical abstract

